Edge Ferromagnetism from Majorana Flat Bands: Application to Split Tunneling-Conductance Peaks in High-T[subscript c] Cuprate Superconductors

Edge Ferromagnetism from Majorana Flat Bands: Application to Split Tunneling-Conductance Peaks in High-T_c Cuprate Superconductors

Andrew C. Potter and Patrick A. Lee
Department of Physics, Massachusetts Institute of Technology, Cambridge, Massachusetts 02139, USA
(Received 1 April 2013; published 20 March 2014)

In mean-field descriptions of nodal d-wave superconductors, generic edges exhibit dispersionless Majorana fermion bands at zero energy. These states give rise to an extensive ground-state degeneracy, and are protected by time-reversal symmetry. We argue that the infinite density of states of these flat bands make them inherently unstable to interactions, and show that repulsive interactions lead to edge ferromagnetism which splits the flat bands. This edge ferromagnetism offers an explanation for the observation of the splitting of zero-bias peaks in edge tunneling in high-T_c cuprate superconductors. We argue that this mechanism for splitting is more likely than previously proposed scenarios and describe its experimental consequences.

DOI: 10.1103/PhysRevLett.112.117002 PACS numbers: 74.72.-h, 74.25.Ha, 74.55.+v, 75.70.Rf

The discovery of topological insulators [1] has led to a reexamination of the role of symmetries for protecting surface states. Since known topological invariants are defined only in the presence of an energy gap, this effort has focused almost exclusively on gapped insulators and superconductors. However, well-defined topologically protected surface states can emerge at the boundary of (noninteracting) gapless systems, so long as translational invariance along the boundary is preserved. For example, in the absence of interactions, clean systems with bulk Dirac nodes, such as graphene [2], Weyl semimetals [3,4], and nodal superconductors [5,6] are all expected to exhibit dispersionless bands that are spatially confined to the edge. In special cases, flat bands can persist in gapless superconductors even in the presence of disorder [7].

These flat edge bands exist in regions of linear size Λ in the boundary-Brillouin zone, and terminate at bulk gapless nodes where the edge states delocalize from the boundary. In superconducting cases, these edge bands are pinned to the Fermi energy as neutral Majorana fermions, giving rise to large ground-state degeneracy, $D \approx 2^{(\Lambda/2\pi)^{d-1}}$, where d is the spatial dimension of the bulk. This corresponds to an extensive ground-state entropy, $S_0 \sim (\Lambda L)^{d-1}$ in violation of the third law of thermodynamics, and also to an infinite density of states at zero energy. Therefore even arbitrarily weak interactions act as a singular perturbation, and play an essential role in determining the true edge-state structure.

In this Letter, we examine the effects of interactions on flat edge bands, focusing specifically on the case of 2D superconductors with nodal $d_{x^2-y^2}$ pairing symmetry, relevant to the cuprate family of high-temperature superconductors. The flatness of the edge states is protected not only by translation symmetry along the edge, but also time-reversal symmetry (TRS). Therefore, a TRS breaking order is required to lift the edge degeneracy.

Evidence for such TRS breaking was found in normal-metal–$YBa_2Cu_3O_{7-\delta}$ (YBCO) tunnel junction experiments. These show a large zero-bias peak at intermediate temperatures [8–11], corresponding to many low-lying states. The peak subsequently splits into two as the sample is cooled [12,13]. Previously proposed explanations [14–16] of this phenomena were based on the point of view that the edge scattering is pair breaking and suppresses the $d_{x^2-y^2}$ parameter near the edge. In principle, this then allows a different, subdominant pairing symmetry to develop near the edge. In particular, s-wave pairing with a relative $\pi/2$ phase to the bulk order parameter $(d + is)$ was suggested to develop near the edge [14,15]. However, the relevance of this scenario to the high-T_c cuprates is questionable, since superconductivity in these materials is widely believed to arise from strong electron-electron repulsion [17–20], which disfavors s-wave pairing [21].

Viewing the zero-bias peak, instead, from the perspective of topological flat bands naturally suggests a different scenario. Namely, since the flat edge bands are spin degenerate, it is natural to suspect that repulsive interactions will produce ferromagnetism (FM) due to exchange forces, in close analogy to quantum Hall FM in flat Landau levels [22]. Here, we confirm this expectation, and show that whereas repulsive interactions disfavor a $d + is$ pairing, arbitrarily weak repulsion favors FM at the edge (even if there is no tendency towards FM in the bulk). We identify tunneling signatures of the edge FM, which can distinguish it from the previously proposed $d + is$ pairing.

Flat edge bands—To set the stage, we review the structure of flat edge bands in the absence of interactions, as previously discussed in [6]. We start by considering the mean-field Hamiltonian of a superconductor with $d_{x^2-y^2}$-pairing written as a tight-binding model on the square lattice. In the absence of an edge, the Hamiltonian can be written in momentum space:

$$H_d = \frac{1}{2}\sum_k \Psi_k^\dagger [\mathcal{H}_0(\mathbf{k})\tau_3 + \mathcal{H}_\Delta(\mathbf{k})\tau_1]\Psi_k,$$
$$\mathcal{H}_0 = -2t(\cos k_a + \cos k_b) - \mu,$$
$$\mathcal{H}_\Delta = -2\Delta_0(\cos k_a - \cos k_b), \quad (1)$$

(see Fig. 1 inset) where $\Psi = (c_{\uparrow,\mathbf{k}}\ c_{\downarrow,-\mathbf{k}}\ c^\dagger_{\downarrow,-\mathbf{k}}\ -c^\dagger_{\uparrow,\mathbf{k}})$. Furthermore, we ignore the effect of phase fluctuations, which will not be important in what follows, and choose Δ_0 to be uniform and real. For convenience, we have chosen units of length such that the lattice spacing is unity, and shifted the chemical potential such that $\mu = 0$ corresponds to half-filling.

In anticipation of introducing an edge along the $\langle 11\rangle$ direction, we rewrite the Hamiltonian in terms of momenta along, $k = (k_a + k_b/2)$, and perpendicular, $k_\perp = (k_a - k_b/2)$, to the edge, where k, $k_\perp \in [-(\pi/\sqrt{2}), (\pi/\sqrt{2})]$. In these coordinates we have $\mathcal{H}_0 = -2t_k \cos(k_\perp) - \mu$ and $\mathcal{H}_\Delta = 2\Delta_k \sin(k_\perp)$, where $t_k = 2t\cos k$ and $\Delta_k = 2\Delta_0 \sin k$.

Next, we introduce an edge. Though any direction misaligned from $\langle 10\rangle$ will exhibit edge bands, for concreteness we consider an edge along the $\langle 11\rangle$ direction. Since $k_\perp$ is no longer a good quantum number, one must move to a real-space description for the y direction. For each value of k, the Hamiltonian is formally identical to an effective 1D tight-binding chain with hopping t_k and p-wave pairing Δ_k.

It is well known [23] that such 1D wires with p-wave pairing exhibit zero-energy Majorana end states so long as $|2t_k| < |\mu|$ and $\Delta(k) \neq 0$. In the present case, there will be a Majorana zero mode for each $|k| < \cos^{-1}(\mu/4t)$, $k \neq 0$. These edge bands terminate at bulk nodal points, $k = 0$, $\pm\Lambda$, where $\Lambda = \cos^{-1}(\mu/4t)$.

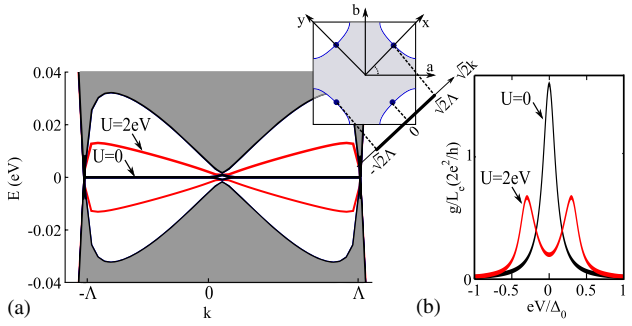

FIG. 1 (color online). (a) Momentum resolved spectrum for the edge for the noninteracting d-wave nodal superconductor for $t = 240$ meV $\Delta_0 = 10$ meV and $U = 0$ (black line, noninteracting) and $U = 2$ eV.(red curves, mean-field). Solid lines indicate edge states and gray, shaded regions represent the bulk continuum. In the presence of interactions the edge becomes ferromagnetic, splitting the flat band of edge states. The small splitting at $k = 0$ is a finite size artifact. The inset shows the 2D Brillouin zone, rotated coordinate system, and projection onto the edge. (b) Edge tunneling conductance with broadening parameter $\gamma_0 = 0.1(U/\pi\xi_0)$, for $U = 0$ (black) and $U = 2$ eV (red).

For k between the bulk nodes, the Majorana end-state operators with momentum k and the z component of spin σ take the form [23,24]

$$\gamma_{k\sigma} \approx \sum_y \phi_k(y)[c_{k\sigma}(y) + i\sigma \mathrm{sgn}(k) c^\dagger_{-k,-\sigma}(y)]. \quad (2)$$

The states at $\pm k$ are not independent, but rather are related by $\gamma_k = -\gamma^\dagger_{-k}\sigma_y$, where $\gamma_k = (\gamma_{k\uparrow}\gamma_{k\downarrow})^T$. This means that the edge states have half as many degrees of freedom as bulk Bogoliubov quasiparticles, which are spinful Dirac fermions, and hence should be regarded as spinful Majorana fermions.

Detailed expressions for the wave function $\phi(y)$ are given in [23] (see also Appendix A in [24]). For our present purposes, the only important feature of these wave functions is their spatial extent, and it is sufficient to use the approximate form $\phi_k(y) \approx (e^{-y/\xi_k}/\sqrt{\xi_k/2})$. The confinement length of the edge wave functions depends on k, diverging as $\xi_k \approx (\xi_0/|k|)$ and $\xi_k \approx (\xi_0^{-1}/|\pm\Lambda - k|)$ near $k \approx 0$, $\pm\Lambda$, respectively, and falling to a minimum of $\xi_k \approx (\xi_0/\Lambda)$ near $k \approx \Lambda(1 - \xi_0^{-2})$. Here $\xi_0 = (t/\Delta_0)$ is the bulk coherence length.

Instability towards FM—We incorporate interactions by an on-site repulsive Hubbard term, $H_U = (U/2)\sum_i n_i(n_i - 1)$, where n_i is the number of electrons on site i. First, we focus only on the subspace of zero-energy edge states to analyze the possible competing instabilities. From this approach, we identify the dominant tendency towards FM. Next, we support this picture by numerically conducting a mean-field analysis that incorporates both surface and bulk states. Because of the absence of quantum fluctuations about the Ferromagnetic ground state we expect the mean-field description to be sufficient at low temperatures, where thermal fluctuations are not important.

Spontaneous symmetry breaking order can endow the flat Majorana edge bands with dispersion. Focusing only on the types of order that preserve translation symmetry, the generic edge dispersion takes the form

$$H_m = \sum_k \gamma_k^\dagger [m_0(k) + \mathbf{m}(k)\cdot\boldsymbol{\sigma}]\gamma_k, \quad (3)$$

where $m_\mu \in \mathbb{R}$, and $\boldsymbol{\sigma}$ are spin Pauli matrices.

The transformation properties of $M_{ab} = m_0\delta_{ab} + \mathbf{m}\cdot\boldsymbol{\sigma}_{ab}$ allow us to identify the physical meaning of the various terms in H_m. Hermiticity requires $M = M^\dagger$. In contrast, time reversal acts on M as $\mathcal{T}(M) = -M^\dagger$, indicating that $H_m \neq 0$ necessarily breaks TRS. Spin rotations, $\gamma \to U\gamma = e^{-i\boldsymbol{\theta}\cdot\boldsymbol{\sigma}}\gamma$ with $U \in \mathrm{SU}(2)$, have the effect $M \to U^\dagger M U$. Finally, under spatial inversions, $x \to -x$, M transforms as like $\mathcal{P}(M) = -\sigma^y M^T \sigma^y$. These considerations show that m_0 and $\mathbf{m}$ break inversion and spin-rotation symmetry, respectively, allowing us to identify $m_0 \neq 0$ with the $d + is$ wave pairing, and $\mathbf{m} \neq 0$ with the edge FM (see Appendix C in [24] for an explicit derivation).

We write the Hubbard U term as $H_U = -(U/2)\sum_{\mathbf{r}}[(n_{\uparrow,\mathbf{r}} - n_{\downarrow,\mathbf{r}})^2 - (n_{\uparrow,\mathbf{r}} + n_{\downarrow,\mathbf{r}})]$, and focus on configurations that are uniform along x. Decomposing the spin density purely in terms of the edge states, $\sum_x (n_{\uparrow,\mathbf{r}} - n_{\downarrow,\mathbf{r}}) \approx \sum_{k,y} |\phi_k(y)|^2 \gamma_k^\dagger \sigma^z \gamma_k + \cdots$, where $(\cdots)$ denotes the remaining contributions from bulk states, gives

$$H_U \approx -\sum_{k,k'} V_{kk'} (\gamma^\dagger \sigma^z \gamma)_k (\gamma^\dagger \sigma^z \gamma)_{k'} + \cdots, \tag{4}$$

where $V_{kk'} \approx (U/2)\sum_y |\phi_k(y)|^2 |\phi_{k'}(y)|^2 \approx (U/\xi_k + \xi_{k'})$. Here we see that it is energetically favorable to have $\langle \gamma^\dagger \sigma^z \gamma \rangle \neq 0$, i.e., to magnetically polarize the edge. A similar analysis started by rewriting H_U in terms of the s-wave pairing order parameter, $H_U \approx +\sum_{kk'} V_{kk'} (\gamma^\dagger \gamma)_k, (\gamma^\dagger \gamma)_{k'}$, shows, as expected, that it is energetically costly to form s-wave pairing at the edge.

Further insight into the ferromagnetic edge instability can be gained by developing a Ginzburg-Landau free energy for the edge magnetization. Ignoring, for the moment, the bulk states, the effective action for the edge-Majorana bands (in imaginary frequency) is $S_\gamma = \frac{1}{2}\sum_{\omega,k} \gamma^\dagger_{\omega,k} (-i\omega) \gamma_{\omega,k} + H_U$. Introducing the Hubbard-Stratonivich field $m_k \sim \sum_{k'} V_{kk'} (\gamma^\dagger \sigma^z \gamma)_{k'}$ to decompose the quartic term, and integrating out the Majorana edge states, we find (see Appendix D in [24])

$$S_{\text{eff}} = \frac{1}{2}\sum_{kk'} m_k (V^{-1})_{kk'} m_{k'} - \sum_k |m_k|. \tag{5}$$

The unusual, nonanalytic $|m_k|$ term arises from the edge bands' singular density of states in the absence of FM order. This term favors $m \neq 0$, even for arbitrarily weak interactions. The saddle point solution $(\delta S_{\text{eff}}/\delta m_k) = 0$ is $m_k = \sum_{k'} V_{kk'}$. The edge-state dispersion is

$$m_k \approx \frac{U}{\pi \xi_0} |k| \left[\Lambda + |k| \log\left(\frac{|k|}{\Lambda + |k|} \right) \right]. \tag{6}$$

The above estimates give $m_{k_{\max}} \approx \Delta_0$. However, this is an overestimate for several reasons. First, disorder will extrinsically broaden the surface bands, smearing out the singular density of states and weakening the instability towards FM. Second, edge roughness will further suppress the pairing near the edge, increasing the confinement lengths ξ_k, and weakening the residual interactions compared to the clean case. Lastly, we have so far ignored the mixing between surface and bulk states induced by the magnetic order. This is justified only for small splitting ($m_k \ll \Delta_k$).

For larger splitting, the dependence of the confinement length on the splitting must be self-consistently taken into account, $\xi_k \sim (v_\perp(k)/\Delta_k - m_k)$, limiting the effects of interactions for large m_k. The bulk states repel the surface bands, keeping them inside the gap, even for arbitrarily large U. These effects can be accounted for by numerically simulating the full bulk plus edge problem using Eq. (1) in the presence of an on-site repulsive $H_U = U\sum_i n_i(n_i - 1) \approx -(U/2)\sum_i m_i c_i^\dagger \sigma^z c_i$ subject to the self-consistency constraint $m_i = \langle c_{ia}^\dagger \sigma^z_{ab} c_{ib} \rangle$ (note that we allow the mean-field parameters to have arbitrary spatial variation in the direction perpendicular to the edge). Representative results using reasonable values of t, U, Δ_0 are shown in Fig. 1.

Our mean-field treatment predicts the dominant weak coupling instability towards edge FM. However, given the absence of an accurate microscopic theory of high-T_c superconductivity, whether this conclusion extends to the strongly correlated regime relevant to real high-T_c cuprate materials is ultimately a matter for experiments to resolve. Consequently, we devote the remainder of the Letter to elucidating experimental consequences of the edge-FM scenario.

Tunneling signatures—The edge bands and ferromagnetic splitting can be revealed by tunneling [8–10,14,15]. At zero temperature, each edge mode contributes a Lorentzian peak centered at bias $\text{eV} = \pm m_k$, with height $2e^2/h$ and width $\gamma_k \approx (\gamma_0/\xi_k) \approx \gamma_0 |k|$. Here, $\gamma_0 \equiv \pi \nu(0) |\Gamma|^2$ is the typical level broadening due to coupling to the metallic lead, where $\nu(0)$ is the density of states of the metallic lead, and Γ is the lead-superconductor tunneling amplitude. We have calculated the detailed tunneling conductance based on a mean-field treatment of H_U and Eq. (1). The results are in agreement with the analytic considerations presented above.

The tunneling conductance from the edge bands, normalized to the length of the edge, is shown in Fig. 1(b). For weak tunneling, $\gamma_0 \ll 1$, the edge-state contribution to the tunneling conductance at bias voltage V is given by

$$g(\text{eV}) = \frac{2e^2}{h} \frac{\gamma_0 L_e}{2\xi_0} \frac{k(\text{eV})}{v_e(\text{eV})}, \tag{7}$$

where L_e is the length of the edge, $k(\varepsilon)$ is the momentum of the edge state with splitting ε (defined by $m_{k(\varepsilon)} = \varepsilon$), and $v_e(\varepsilon) = |\partial m_k/\partial k|_{m_k = \varepsilon}$ is the corresponding edge velocity. The conductance exhibits a peak near the maximal energy splitting $m_{k_{\max}}$, where v_e flattens out providing the large edge-mode density of states that have a comparatively large weight near at edge. The width of this peak is proportional to γ_0.

Parallel magnetic field—An applied magnetic field $\mathbf{H}$ induces further TRS breaking perturbations and further splits the edge states (see Appendix F in [24] for more details). We first consider the simpler case of an in-plane magnetic field, which affects the edge states through the Zeeman coupling, $\mathcal{H}_Z = -(g\mu_B/2)\mathbf{H} \cdot \sum_i c_i^\dagger \boldsymbol{\sigma} c_i \approx (g\mu_B/2)\mathbf{H} \cdot \sum_k \gamma_k^\dagger \boldsymbol{\sigma} \gamma_k$. In the FM scenario described above, this Zeeman energy simply adds to the spontaneous zero-field splitting, further splitting the edge bands and tunneling peak [see Figs. 2(a) and 2(c), and Fig. 3(a)]. In fact,

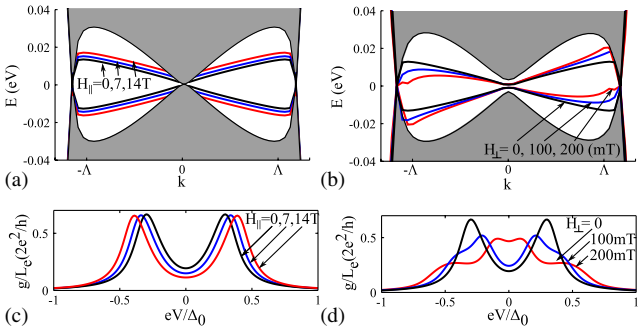

FIG. 2 (color online). A magnetic field further splits the edge bands, and corresponding tunneling peak. Panels (a) and (b) show the edge spectrum (solid lines) and projected bulk spectrum (gray shaded regions) for parallel (in the a-b plane) and perpendicular (along the c axis) magnetic fields. (c),(d) show the corresponding tunneling conductance from the edge states, obtained from a numerical mean-field analysis. Black, blue, and red curves correspond to $H_{\|} = 0$, 7, and 14 T for (a),(c), and to $H_{\perp} = 0$, 100, and 200 mT for (b),(d).

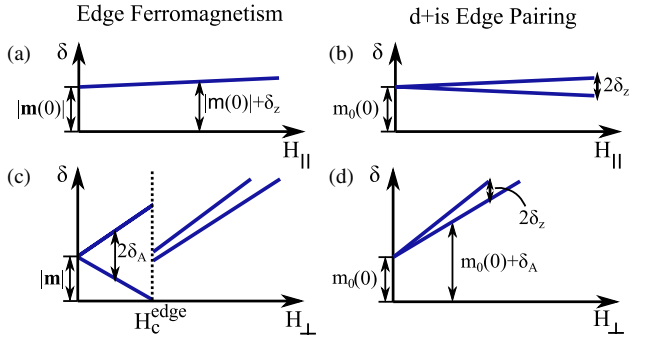

FIG. 3 (color online). Schematic dependence of the tunneling peak position δ on magnetic field, for edge-FM [panels (a),(c)] and $d + is$ [panels (b),(d)] scenarios. Only the positive bias peak is shown here (negative bias is symmetric). The top (a),(b) and bottom (c),(d) rows show the effects of parallel and perpendicular fields, respectively. The dashed line denotes a first-order phase transition where the spontaneous edge FM is destroyed by the applied field. δ_Z and δ_A are, respectively, the splittings induced by the Zeeman energy and orbital screening currents from the external field.

such a splitting of the tunneling peak with an in-plane field, with a slope equal to the Zeeman splitting, has been observed [13].

In contrast, no such splitting is expected for the previously suggested scenario in which the zero-field splitting is due to $d + is$ pairing near the edge [14,15]. Spontaneous $d + is$ edge pairing corresponds to an m_0 type mass [see Eq. (3)] at zero field. Applying an in-plane field induces an $\mathbf{m}$-type term, which further splits the tunneling peak into four [see Fig. 3(b)]. However, the further splitting occurs symmetrically about the zero-field peak position, and there will be no shift in the average peak position. Consequently, the in-plane field data of [13] provides evidence for spontaneous FM rather than a subdominant TR breaking pairing.

Perpendicular magnetic field—In addition to Zeeman effects, a magnetic field $H_{\perp}$, perpendicular to the a-b plane, will produce orbital screening currents. These introduce the edge perturbation, $\mathcal{H}_A = \int \mathbf{A} \cdot \mathbf{j} \approx \sum_k m_0(k) \gamma_k^{\dagger} \gamma_k$. Here $\mathbf{A} = \lambda_L H e^{-y/\lambda_L} \hat{\mathbf{x}}$ is the vector potential corresponding to uniform perpendicular field H (in the unitary gauge), $\mathbf{j}$ is the electron current, and $m_0(k) = \int dy A(y) |\phi_k(y)|^2 \approx (H/H_c)\Delta(k)$. λ_L is the London penetration depth, $H_c = (\Phi_0/\pi\xi_0\lambda_L)$ is the thermodynamic critical field, and $\Phi_0 = (hc/2e)$ is the superconducting flux quantum. For YBCO, $H_c \approx 1T$. Note that, in the presence of vortices, $\mathbf{A}$ should be replaced by $\mathbf{A} - (c/2e)\nabla\theta$ in the above expression, where θ is the superconducting phase.

For $H < H_c$, the screening currents from $H_{\perp}$, induce an m_0-type term that, in the FM scenario, shifts the $k > 0$ and $k < 0$ edge-state energies in opposite directions [see Fig. 2(c)], leading to a fourfold split tunneling peak [see Fig. 2(d) and Fig. 3(c)]. As H is increased beyond $H_c^{\text{edge}} \approx$ 250 mT the negative energy spin-down states are pulled above the chemical potential, and the spontaneous edge FM is killed in a first-order field-induced phase transition. Past this point, the tunneling conductance shows only a twofold split tunneling peak, centered at $\text{eV} \approx \pm(H/H_c)\Delta_0$. Simulated tunneling conductance from a mean-field treatment of Eq. (1) with H_U, $\mathcal{H}_A$, and $\mathcal{H}_Z$ agree with the schematic picture presented in Fig. 3. In addition, the perpendicular field simulations show a very broad peak for $H > H_c^{\text{edge}}$ (see Appendix F in [24]).

In contrast, for the previously suggested $d + is$ scenario, the orbital currents simply add to the zero-field splitting [see Fig. 3(d)]. Therefore, in principle, the effects of a perpendicular field on tunneling conductance can provide further evidence to distinguish the FM and $d + is$ scenarios. There is insufficient data from [12,13] at low fields, to discern whether there is first-order transition in the perpendicular field at $H_{\perp} = H_c^{\text{edge}}$. It is also possible that our estimate of H_c^{edge} is inaccurate due to vortex pinning effects. There are other complications in the data which are not accounted for in our simple model. The peak shift saturates at large $H_{\perp}$; however, the previously proposed explanation based on nonlinear saturation of the Meissner currents [15,25] is also applicable to our scenario. There are also complicated hysteresis effects in the perpendicular field which are not easy to explain [27]. For these reasons, we suggest that the parallel field dependence provides simpler, and more easily interpreted evidence.

Discussion—We have shown that the topological flat bands provide a useful perspective for discussing TRS breaking at the edge of high-T_c cuprate superconductors. This viewpoint naturally suggests an instability towards ferromagnetic order from repulsive interactions. The magnetic-field dependence of tunneling peak splitting provides a simple, though indirect, experimental test to distinguish the

proposed FM order from previously proposed $d + is$ pairing [14,15]. Alternatively spin-polarized planar-tunneling or STM measurements would enable one to directly detect of the predicted FM order.

In closing, we remark that flat Majorana bands are also expected to appear in certain classes of nodal spin-triplet superconductors [7]. In contrast to the d-wave case discussed here, these edge bands would not be spin degenerate, and more complicated types of (incommensurate density-wave) order are required. Moreover, unlike the ferromagnetic case discussed here, quantum fluctuations would generically destroy the density-wave order leaving only power-law correlations.

We thank Liang Fu for helpful discussions, and acknowledge funding from DOE Grant No. DEFG0203ER46076.

[1] M. Z. Hasan and C. L. Kane, Rev. Mod. Phys. **82**, 3045 (2010).
[2] M. Fujita, K. Wakabayashi, K. Nakada, and K. Kusakabe, J. Phys. Soc. Jpn. **65**, 1920 (1996).
[3] S. Murakami, New J. Phys. **9**, 356 (2007).
[4] Xiangang Wan, A. M. Turner, A. Vishwanath, and S. Y. Savrasov, Phys. Rev. B **83**, 205101 (2011).
[5] C.-R. Hu, Phys. Rev. Lett. **72**, 1526 (1994).
[6] F.Wang and D. H. Lee, Phys. Rev. B **86**, 094512 (2012).
[7] C. L. M. Wong, J. Liu, K. T. Law, and P. A. Lee, Phys. Rev. B **88**, 060504(R)(2013).
[8] J. Geerk, X. X. Xi, G. Linker, Z. Phys. B **73**, 329 (1988).
[9] J. Lesueur, L. H. Greene, W. L. Feldmann, and A. Inam, Physica (Amsterdam) **191C**, 325 (1992).
[10] M. Covington, R. Scheuerer, K. Bloom, and L. H. Greene, Appl. Phys. Lett. **68**, 1717 (1996).
[11] Y. Tanaka and S. Kashiwaya, Phys. Rev. Lett. **74**, 3451 (1995).
[12] M. Covington, M. Aprili, E. Paraoanu, L. H. Greene, F. Xu, J. Zhu, and C. A. Mirkin, Phys. Rev. Lett. **79**, 277 (1997).
[13] R. Krupke and G. Deutscher, Phys. Rev. Lett. **83**, 4634 (1999).
[14] M. Matsumoto and H. Shiba, J. Phys. Soc. Jpn. **64**, 3384 (1995); J. Phys. Soc. Jpn. **64**, 4867 (1995).
[15] M. Fogelstrom, D. Rainer, and J. A. Sauls, Phys. Rev. Lett. **79**, 281 (1997).
[16] C. Honerkamp, K. Wakabayashi, and M. Sigrist, Europhys. Lett. **50**, 368 (2000).
[17] P. A. Lee, N. Nagaosa, and X.-G. Wen, Rev. Mod. Phys. **78**, 17 (2006).
[18] D. J. Scalapino, Phys. Rep. **250**, 329 (1995); C. J. Halboth and W. Metzner, Phys. Rev. Lett. **85**, 5162 (2000).
[19] T. A. Maier, M. Jarrell, T. C. Schulthess, P. R. C. Kent, and J. B. White, Phys. Rev. Lett. **95**, 237001 (2005).
[20] A. I. Lichtenstein and M. I. Katsnelson, Phys. Rev. B **62**, R9283 (2000); S. S. Kancharla, B. Kyung, D. Senechal, M. Civelli, M. Capone, G. Kotliar, and A.-M. S. Tremblay, Phys. Rev. B **77**, 184516 (2008).
[21] It was also suggested [15] that a more exotic g-wave pairing with eight nodes could be favored by a spin-fluctuation mediated pairing produced by repulsion. However, we expect the $d + ig$ edge pairing to be less favorable than the FM proposed here since (1) the presence of extra nodes reduces the pairing energy gain, and (2) this high-angular-momentum pairing is very susceptible to pair breaking from impurities and edge roughness.
[22] See, for example, K. Nomura and A. H. MacDonald, Phys. Rev. Lett. **96**, 256602 (2006).
[23] A. Kitaev, Phys. Usp. **44**, 131 (2001)
[24] See Supplemental Material at http://link.aps.org/supplemental/10.1103/PhysRevLett.112.117002 for more details on the properties of the edge states, their symmetries, and a derivation of the effective Ginzburg-Landau action.
[25] S. K. Yip and J. A. Sauls, Phys. Rev. Lett. **69**, 2264 (1992).
[26] C. P. Bean and J. D. Livingston, Phys. Rev. Lett. **12**, 14 (1964).
[27] Reference [13] proposes an explanation of this hysteresis based on a surface barrier to vortices flowing in or out of the sample [26]. However, it is unclear to us how these barrier effects can explain the direction and other details of the hysteresis loop observed in [13]. In particular, contrary to the arguments presented in [13], the typical supercurrent near the edge is expected to increase linearly with the applied field, $j_{\text{edge}} \approx (H_{\perp}/\lambda_L)$, independently of whether or not there are vortices in the sample (see Appendix F.1 in [24]).